Estimates for temperature in projectile-like fragments in geometric and transport models

S. Mallik,[1] S. Das Gupta,[2] and G. Chaudhuri[1]
[1]*Theoretical Physics Division, Variable Energy Cyclotron Centre, 1/AF Bidhan Nagar, Kolkata 700064, India*
[2]*Physics Department, McGill University, Montréal H3A 2T8, Canada*
(Received 8 September 2013; revised manuscript received 28 January 2014; published 25 April 2014)

Projectile-like fragments emerging from heavy ion collision have an excitation energy which is often labeled by a temperature. This temperature was recently calculated using a geometric model. We expand the geometric model to include dynamic effects using a transport model. The calculated temperatures agree quite well with values of temperature needed to fit experimental data.

DOI: 10.1103/PhysRevC.89.044614 PACS number(s): 25.70.Mn, 25.70.Pq

I. INTRODUCTION

Projectile multifragmentation is a practical tool for producing exotic nuclei in the laboratory and remains a very active field of research both experimentally and theoretically. This theoretical paper deals with dynamic effects of projectile fragmentation.

There are many theoretical models for projectile multifragmentation, including the statistical multifragmentation model (SMM) [1] (see also Refs. [2] and [3] for application of SMM to projectile fragmentation), heavy-ion phase-space exploration (HIPSE) model [4] (see also Ref. [5] for an application), antisymmetrized molecular dynamics (AMD) model [6] (see also Ref. [5] for applications), the abrasion-ablation model of Gaimard, Schmidt, and Brohm [7,8], and the Empirical parametrization of fragmentation cross sections (EPAX) [9] model.

In recent years we proposed a model [10–12] for projectile fragmentation whose predictions were compared with many experimental data with good success. In contrast with the models mentioned above, our model uses the concept of temperature. The concept of temperature is quite familiar in heavy-ion physics, whether to describe the physics of participants (where the temperature can be very high) or the physics of spectators (where the temperature is expected to be much lower). The "nuclear caloric curve" was much researched as a signature of phase transition in nuclear systems [13,14]. Temperature of an emitting zone is often computed using the Albergo formula [15]. Thus temperature is a useful concept in projectile spectator physics.

Our model has three parts. To start, we need an abrasion cross section. For a given impact parameter, this was calculated using straight-line trajectories for the projectile and the target, leading to definite mass and shape for the projectile-like fragment (PLF). The PLF created will not be at zero temperature. Let us label the mass of the PLF by $A_s(b)$ and the mass of the projectile by A_0. It was conjectured that that the temperature of the PLF is a universal function of the wound $1.0 - A_s/A_0$. This was parametrized as [11]

$$T = 7.5\ \text{MeV} - [A_s/A_0]\,4.5\ \text{MeV}. \quad (1)$$

A select set of experimental data from Sn-Sn collisions [2] were used in Ref. [11] to arrive at the numbers above. The formula was seen to give very reasonable fits for many experimental data not only for Sn-Sn but other pairs of ions also. The objective of the present work is to investigate if we can arrive at the numbers generated by this simple parametrization from a microscopic theory. We may call this temperature the primordial temperature. The complete model does not stop here, of course, and many more steps are needed to calculate observables. We then postulate that this hot nuclear system will expand and break up into all possible composites dictated solely by phase space. This is the canonical thermodynamic model (CTM) [16]. The resulting hot composites will further evolve by two-body sequential decays, leading to the final products measured by experiments. Experimental results for many pairs of ions in the beam energy range 140 MeV/nucleon to 1 GeV/nucleon were fitted quite well by this model [11,12].

Our objective here is to estimate the value of the temperature of the PLF when it is formed. We estimated this in a geometric model [17]. As the numerical methods used for the geometric model will be extended to a dynamical transport model, we need to review the geometric model first. Conceptually the geometric model is simple but the calculations are nontrivial. We assume that the size and shape of the PLF is given by straight-line cuts and that divisions between participants and spectators are very clean. This excludes low beam energy. Experiments at Michigan used 140 MeV/nucleon. We made an *ad hoc* assumption that we can use straight-line cuts at this beam energy, and higher and lower energies were not attempted. In the geometric model, some parts of the projectile are removed, which leaves the PLF with a crooked shape. Nuclear structure effects ascribe to this shape an excitation energy. We now use the CTM [16]. In that model, for a given mass and temperature one can compute the excitation energy per nucleon. We reverse the procedure to go from excitation energy to temperature. Note that in the geometric model the beam energy does not enter the calculation; the only assumption is that it is large enough for straight-line trajectories to be valid.

In later sections we estimate the PLF temperature from a transport model Boltzmann-Uehling-Uhlenbeck (BUU) calculation. These are the principal results of this work. These calculations can be used for many purposes but we restrict ourselves only to the objective of trying to deduce a temperature for the PLF.

II. THE GEOMETRIC MODEL

Calculations with the geometric model were reported in a recent paper [17]. As the tecniques used in the model can be straightforwardly extended to transport model calculations, we describe this briefly, mostly to establish notation and formulas that we need later. The idea of the model is this: When two heavy ions collide, the overlapping parts form the participant zone, leaving a projectile-like spectator and a target-like spectator. Here we are only interested in the PLF. The size and shape of the PLF are taken using straight-line cuts. What are the mass and the energy of this object?

We start by choosing an impact parameter and boost one nucleus in its ground state toward the other nucleus, also in its ground state. We use Thomas-Fermi (TF) solutions for ground states. The kinetic energy density is given by

$$T(\vec{r}) = \int d^3p f(\vec{r},\vec{p}) p^2/2m, \tag{2}$$

where $f(\vec{r},\vec{p})$ is the phase space density. In the ground state of a spherical nucleus we have

$$f(r,p) = \frac{4}{h^3}\theta[p_F(r,p) - p]. \tag{3}$$

This leads to

$$T = \frac{3h^2}{10m}\left[\frac{3}{16\pi}\right]^{2/3} \int \rho(r)^{5/3} d^3r. \tag{4}$$

For potential energy we take

$$V = A\int d^3r \frac{\rho^2(r)}{2} + \frac{1}{\sigma+1} B \int \rho^{\sigma+1}(r) d^3r + \frac{1}{2}\int d^3r d^3r' v(\vec{r},\vec{r}')\rho(\vec{r})\rho(\vec{r}'). \tag{5}$$

The first two terms are usual zero-range Skyrme interactions; the third term is a finite-range interaction which is needed to generate a diffuse (as opposed to a sharp) surface. This term also makes the energy shape dependent. Numerical methods of constructing TF solutions with such forces are given in Ref. [18]. For the calculations that follow, we model the phase-space density of the TF solution by choosing test particles with appropriate positions and momenta using Monte Carlo simulations [19]. In most of this work we consider 100 test particles ($N_{\rm test} = 100$) for each nucleon.

Thomas-Fermi solutions for relevant nuclei were constructed with following force parameters: The constants A, B, and σ [Eq. (4)] were taken to be $A = -1533.6$ MeV fm^3, $B = 2805.3$ MeV fm$^{7/2}$, and $\sigma = 7/6$. For the finite-range potential we chose a Yukawa: V_y.

$$V_y = V_0 \frac{e^{-|\vec{r}-\vec{r}'|/a}}{|\vec{r}-\vec{r}'|/a}, \tag{6}$$

with $V_0 = -668.65$ MeV and $a = 0.45979$ fm. These have been used in the past to construct TF solutions which collide in heavy-ion collisions [20].

We use the method of test particles to evaluate excitation energies of a PLF with any given shape. A PLF can be constructed by removing a set of test particles. Which test particles will be removed depends upon collision geometry envisaged. For example, consider central collision of ^{58}Ni on ^{9}Be. Let z to be the beam direction. For impact parameter $b = 0$ we remove all test particles in ^{58}Ni whose distance from the center of mass of ^{58}Ni has $x^2 + y^2 < r_9{}^2$ where $r_9 = 2.38$ fm is the half radius of ^{9}Be. The cases of nonzero impact parameters can be similarly considered.

We point out that this procedure of removing test particles from the projectile may produce an error if the target is small and/or for very peripheral collisions even if both the target and the projectile are heavy. There can be transparency when small amounts of nuclear matter are traversed. However, this prescription of removing test particles from the projectile when they are in the way of the target produces very definite predictions. The transparency problem is treated well in the transport model that we discuss later.

Continuing with the geometric model, we have now obtained the PLF by removing some test particles as described above. Evaluating the mass number and kinetic energy is straightforward [17]. Evaluating potential energy requires much more work. We need a smooth density to be generated by positions of test particles. We use the method of Lenk and Pandharipande to obtain this smooth density. Other methods are possible [19]. Experience has shown that Vlasov propagation with Lenk-Pandharipande prescription conserves energy and momenta very well [21]. For the geometric model time propagation is not needed. We will need that for BUU calculations in later sections.

The configuration space is divided into cubic lattices. The lattice points are l fm apart. Thus the configuration space is discretized into boxes of size l^3 fm^3. Density at lattice point r_α is defined by

$$\rho_L(\vec{r}_\alpha) = \sum_{i=1}^{AN_{\rm test}} S(\vec{r}_\alpha - \vec{r}_i). \tag{7}$$

The form factor is

$$S(\vec{r}) = \frac{1}{N_{\rm test}(nl)^6} g(x)g(y)g(z), \tag{8}$$

where

$$g(q) = (nl - |q|)\Theta(nl - |q|). \tag{9}$$

The advantage of this form factor is detailed in Ref. [21] so we do not discuss it here. In this work we have always used $l = 1$ fm and $n = 1$.

It remains to state how we evaluate the potential energy term [Eq. (5)]. The zero-range Skyrme interaction contributions are very simple. For example, the first term is calculated by using

$$A\int d^3r \frac{\rho^2(r)}{2} = A\sum_\alpha (l^3)\rho_L^2(r_\alpha)/2. \tag{10}$$

With our choice $l^3 = 1$ fm^3. The third term in Eq. (5) (the Yukawa term) is rewritten as $1/2\sum_\alpha \rho_L(\vec{r}_\alpha)\phi_L(\vec{r}_\alpha)$, where $\phi(\vec{r})$ is the potential at $\vec{r}$ due to the Yukawa, i.e., $\phi(\vec{r}) = \int V_y(|\vec{r}-\vec{r}'|)\rho(r')d^3r'$.

The calculation of Yukawa (and/or Coulomb) potential due to a charge distribution which is specified at points of cubic lattices is very nontrivial and involves iterative procedure. This

has been used a great deal in applications involving time-dependent Hartree-Fock theory [22–25].

With this method we can calculate the total energy of the PLF. However, we are interested in excitation energy of the system, which requires us to find the ground-state energy of the PLF, which has lost some nucleons from the projectile. We can use TF theory to find this. Knowing the mass number and the excitation energy, we use the CTM [16] to deduce the temperature. Results of the geometric model can be found in a recent publication [17]. We show some results in the next two sections.

III. TRANSPORT MODEL: CALCULATIONS I

We begin transport model calculations to identify and investigate properties of PLF. Two nuclei in their Thomas-Fermi ground states are boosted towards each other with appropriate velocities at a given impact parameter. We choose to calculate first ^{58}Ni on ^{9}Be, which was experimentally investigated at Michigan State University (MSU) with beam energy of 140 MeV/nucleon. The calculations here follow the guidelines of Ref. [19] but some details are altered. Two-body collisions are calculated as in Appendix B of Ref. [19], except that pion channels are closed, as here we are interested only in spectator physics (pions are created in the participants). In addition, for collision at 140 MeV/nucleon, pion production in the participant zone should be minuscule. At 600 MeV/nucleon, the highest beam energy we have used there could have some spillover effect. We estimate the effect at the end of Sec. IV. The mean field is that prescribed in Sec. II: zero-range Skyrme plus the Yukawa of Eq. (6). The potential energy density is

$$v[\rho(\vec{r})] = \frac{A}{2}\rho^2(\vec{r}) + \frac{B}{\sigma+1}\rho^{\sigma+1}(\vec{r}) + \frac{1}{2}\rho(\vec{r})\phi(\vec{r}), \quad (11)$$

where $\phi(\vec{r})$ is the potential generated by the Yukawa: $\phi(\vec{r}) = \int V_y(|\vec{r}-\vec{r'}|\rho(\vec{r'})d^3r'$. The Vlasov part is done as in Eqs. (2.14a) and (2.14b) of Ref. [21]:

$$\dot{\vec{r}}_i = \frac{\partial H}{\partial \vec{p}_i} = \frac{\vec{p}_i}{m}, \quad (12)$$

$$\dot{\vec{p}}_i = -N_{\rm test}\sum_\alpha \frac{\partial V}{\partial \rho_\alpha}\vec{\nabla}_i\rho_\alpha, \quad (13)$$

where V is the total potential energy of the system. The Lenk-Pandharipande method is necessary here as all other known (to us) methods have numerical uncertainties in energy evaluation which can hide the effects we are after. The number of test particles to represent the phase space is 100 per nucleon.

We exemplify our method with collision at impact parameter $b = 4$ fm. It is useful to work in the projectile frame and set the target nucleons with the beam velocity in the negative z direction. Figure 1 shows the test particles at $t = 0$ fm/c (when the nuclei are separate), $t = 10$ fm/c, $t = 25$ fm/c, and $t = 50$ fm/c (Be has traversed the original Ni nucleus). The calculation was started with the center of Ni at 25 fm; at the end a large blob remains centered at 25 fm. Clearly this is the PLF. However, a quantitative estimate of the mass of the PLF and its energy requires further analysis. This type of

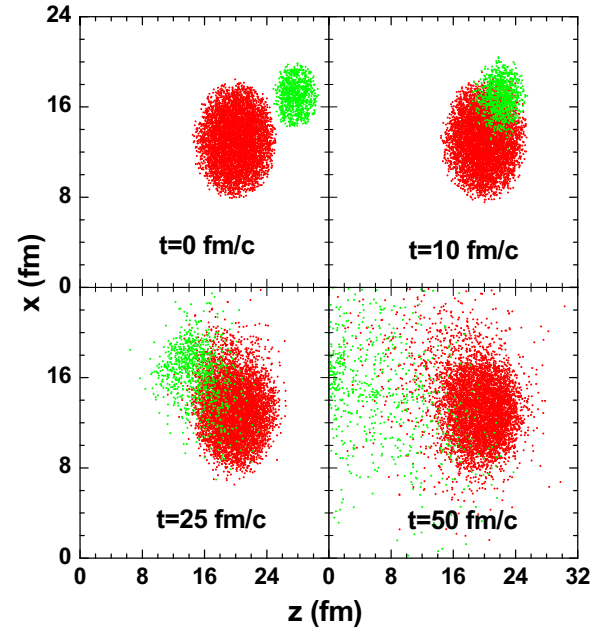

FIG. 1. (Color online) Time evolution of ^{58}Ni (red [gray]) and ^{9}Be (green [gray]) test particles for 140 MeV/nucleon at impact parameter $b = 4$ fm.

analysis was done for each pair of ions and at each impact parameter, and details vary from case to case. We exemplify this in one case only.

For the analysis, it is convenient to introduce a kinetic energy density and a z component of momentum density (we use $p_z c$ rather than p_z). Density at lattice point r_α is defined by

$$\rho_L(\vec{r}_\alpha) = \sum_{i=1}^{AN_{\rm test}} S(\vec{r}_\alpha - \vec{r}_i). \quad (14)$$

For kinetic energy density we use

$$T_L(\vec{r}_\alpha) = \sum_{i=1}^{AN_{\rm test}} T_i S(\vec{r}_\alpha - \vec{r}_i), \quad (15)$$

where T_i is the kinetic energy of the ith test particle. It is also useful to introduce a density for the zth component of momentum:

$$(p_z c)_L(\vec{r}_\alpha) = \sum_{i=1}^{AN_{\rm test}} (p_z c)_i S(\vec{r}_\alpha - \vec{r}_i). \quad (16)$$

The symbol α stands for values of the three coordinates of the lattice point $\alpha = (x_l, y_m, z_n)$. We often, for a fixed value of z_n, sum over x_l, y_m. For example, $\sum_{l,m}\sum_{i=1}^{AN_{\rm test}} S[(x_l y_m z_n) - \vec{r}_i]$ is denoted by $\rho_z(z_n)$, and similarly for kinetic energy or total energy density $T(z_n)$ or $E_T(z_n)$ and for $p_z c(z_n)$, etc.

In Fig. 2 we plot $\rho_z(z)$ as a function of z at $t = 0$ (when the the nuclei start to approach each other) and at $t = 50$ fm/c (when Be has traversed Ni). Figure 3 adds more details to the situation at 50 fm/c. At far right one has the PLF. Progressively towards the left one has the participant zone characterized by a higher energy per nucleon $E_T(z)/\rho_z(z)$ and lower value of

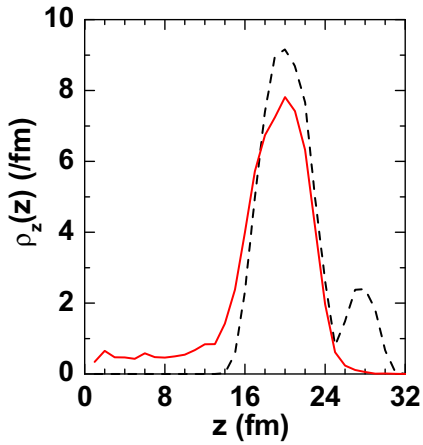

FIG. 2. (Color online) $\rho_z(z)$ variation with z at $t = 0$ fm/c (black dashed line) and 50 fm/c (red [gray] solid line) for 140 MeV/nucleon ^{58}Ni on ^{9}Be reaction studied at an impact parameter $b = 4$ fm.

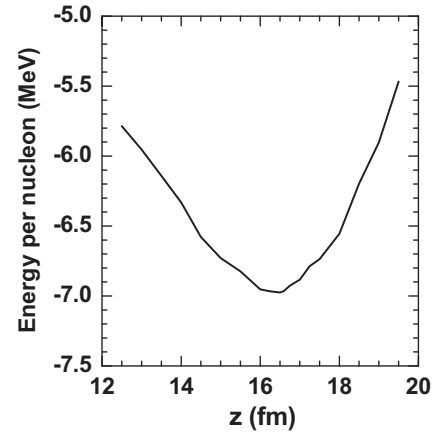

FIG. 4. Energy per nucleon of the system remaining to the right side of a wall at different values of z (see Fig. 3) for 140 MeV/nucleon ^{58}Ni on ^{9}Be reaction at an impact parameter $b = 4$ fm studied at $t = 50$ fm/c.

$p_z c$ per nucleon $[=p_z c(z)/\rho_z(z)]$. Closer to the left edge one has target spectators. In order to specify the mass number and energy per nucleon of the PLF we need to specify which test particles belong to the PLF and which belong to the rest (participant and target spectators). Our configuration box stretches from $z = 0$ to $z = 40$ fm. If we include all test particles in this range we have the full system with the total particle number $67(58 + 9)$ and the total energy of beam plus projectile in the projectile frame. Let us consider constructing a wall at $z = 0$ and pulling the wall to the right. As we pull, we leave out the test particles to the left of the wall. With the test particles to the right of the wall, we compute the number of nucleons and the total energy per nucleon. The number of particles goes down and initially the energy per nucleon will go down also as we are leaving out the target projectiles

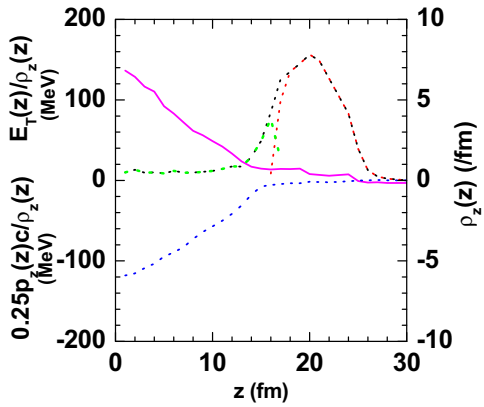

FIG. 3. (Color online) Momentum per nucleon $p_z c(z)/\rho_z(z)$ (blue [gray] dotted line) and total energy per nucleon $E_T(z)/\rho_z(z)$ (magenta [gray] solid line) for 140 MeV/nucleon ^{58}Ni on ^{9}Be reaction at an impact parameter $b = 4$ fm studied at $t = 50$ fm/c. Total density $[\rho_z^t(z)]$, PLF density $[\rho_z^p(z)]$, and remaining part density $[\rho_z^r(z)]$ along the z direction at $t = 50$ fm/c are shown by black, red (gray), and green (gray) dashed lines respectively. For drawing all quantities in the same scale, $p_z c(z)/\rho_z(z)$ is divided by a factor of 4.

first and then the participants. At some point we enter the PLF, and if we pull a bit further we are cutting off part of the PLF, giving it a nonoptimum shape, so the energy per nucleon will rise. The situation is shown in Fig. 4. The point which produces this minimum is a reference point. The test particles to the right are taken to belong to PLF; those to the left are taken to represent the participants and target spectators. Not surprisingly, this point is in the neighborhood where both $E_T(z)/\rho(z)$ and $p_z c/\rho(z)$ flatten out.

The net end results of some of our BUU calculations are presented in Fig. 5. In the upper panel we show results for ^{58}Ni on ^{9}Be at 140 MeV/nucleon. The BUU results are compared with the geometric model results and graph of Eq. (1). As conjectured in Ref. [17], the geometric model results are driven up when dynamics is included. In the lower panel only BUU calculation results are shown for (a) ^{40}Ca on ^{9}Be at 140 MeV/nucleon, (b)^{58}Ni on ^{9}Be at 140 MeV/nucleon, and (c) at 400 MeV/nucleon. We are not aware of any experiments at 400 MeV/nucleon; this was done merely to check if in BUU, PLF physics is sensitive to beam energy. The geometrical model assumes it is not.

IV. TRANSPORT MODEL: CALCULATIONS II

Vlasov propagation with Skyrme plus Yukawa for large ion collisions is not practical. Given nuclear densities on lattice points, one is required to generate the potential which arises from the Yukawa interaction. Standard methods require iterative procedures involving matrices. In the case of Ni on Be, in the early times of the collision, the matrices are of the order of 1000 by 1000: As the system expands the matrices grow in size, reaching about 7000 by 7000 at $t = 50$ fm/c. If we want to do large systems (Sn on Sn, for example) very large computing efforts are required.

To treat large but finite systems we use a mean field Hamiltonian Lenk and Pandharipande devised for finite nuclei. The mean field involves not only the local density but also the derivative of local density up to second order. The derivative

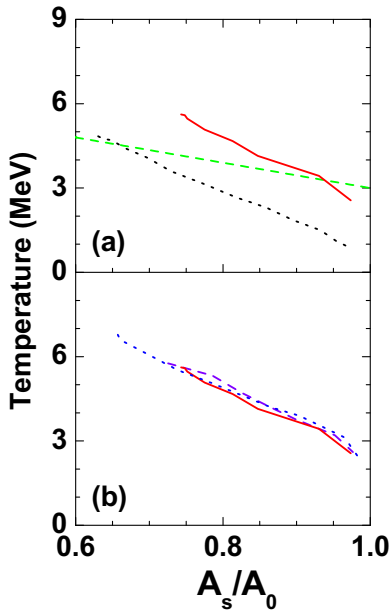

FIG. 5. (Color online) (a) Temperature profile for ^{58}Ni+^{9}Be reaction at 140 MeV/nucleon obtained from BUU model calculation (red [gray] solid line) compared with that calculated from general formula [Eq. (1)] (green [gray] dashed line) and geometrical model (black dotted line). (b) Temperature profiles obtained from BUU calculation for ^{40}Ca+^{9}Be reaction at 140 MeV/nucleon (violet [gray] dashed line) and ^{58}Ni+^{9}Be reaction at 140 MeV/nucleon (red [gray] solid line) and at 400 MeV/nucleon (blue [gray] dotted line).

terms do not affect nuclear matter properties but in a finite system it produces quite realistic diffuse surfaces and liquid-drop binding energies.

In order to keep the same notation as used in previous sections, we write the Lenk-Pandharipande mean field as follows. The mean field potential is

$$u[\rho(\vec{r})] = A\rho(\vec{r}) + B\rho^{\sigma}(\vec{r}) + \frac{c}{\rho_0^{2/3}}\nabla_r^2\left[\frac{\rho(\vec{r})}{\rho_0}\right]. \quad (17)$$

The potential energy density is

$$v[\rho(\vec{r})] = \frac{A}{2}\rho^2(\vec{r}) + \frac{B}{\sigma+1}\rho^{\sigma+1}(\vec{r}) + \frac{c\rho_0^{1/3}}{2}\frac{\rho(\vec{r})}{\rho_0}\nabla_r^2\left[\frac{\rho(\vec{r})}{\rho_0}\right]. \quad (18)$$

Since there is no Yukawa term, the values of A and B and possibly σ need to be changed from the values used in Sec. II (and the previous section) to keep the property of nuclear matter unchanged. For calculations reported in this section the values are $A = -2230.0$ MeV fm^3, $B = 2577.85$ MeV fm$^{7/2}$,$\sigma = 7/6$. These values are taken from a previous work [14]. The value of the constant ρ_0 is 0.16 fm^{-3} and the value of constant c is -6.5 MeV.

The next problem is to find the ground-state energy of a nucleus with A nucleons. Here we have used a variational method. A parametrization of realistic density distribution was given by Myers, which has been used many times for heavy-ion

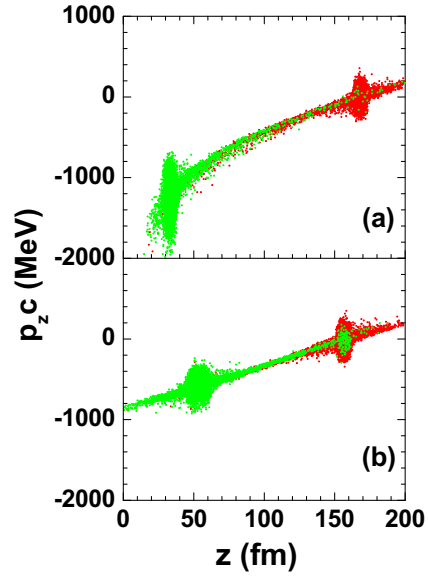

FIG. 6. (Color online) $p_z c$ vs z variation of projectile (red [gray]) and target (green [gray]) test particles at $t = 200$ fm/c for ^{124}Sn on ^{119}Sn reaction studied at an impact parameter $b = 8$ fm with energy (a) 600 MeV/nucleon (relativistic kinematics) and (b) 200 MeV/nucleon (nonrelativistic kinematics).

collisions [18,26,27]. This parametrization is

$$\rho(r) = \rho_M\left[1 - \left(1 + \frac{R}{a}\right)\exp(-R/a)\frac{\sinh(r/a)}{r/a}\right], \quad r < R, \quad (19)$$

$$\rho(r) = \rho_M[(R/a)\cosh(R/a) - \sinh(R/a)]\frac{e^{-r/a}}{r/a}, \quad r > R. \quad (20)$$

There are two parameters here: a, which controls the width of the surface and ρ_M(or R), which controls the equivalent sharp radius. The distribution satisfies $4\pi\int_0^\infty \rho(r)r^2dr = A = \frac{4\pi}{3}\rho_M R^3$. Thus no special normalization is required. The distribution has the advantage that equivalent sharp radius R is simply proportional to $A^{1/3}$ while the half-density radius of a Fermi distribution does not have this simple proportionality. Comparison with Fig. 2 in Ref. [21] shows that the energy calculated by this variational calculation is quite close to what is given by Thomas-Fermi theory.

We do two cases of large colliding systems with the Lenk-Pandharipande mean fields: ^{124}Sn on ^{119}Sn and ^{58}Ni on ^{181}Ta. For these large colliding systems we reduced the number of test particles per nucleon from 100 to 50; $N_{\rm test} = 50$. Figure 6 shows scatter of test particles in the $z, p_z c$ plane for Sn on Sn at time $t = 200$ fm/c for beam energy 200 MeV/nucleon and impact parameter 8 fm/c. The plot, as before, is in the projectile frame and identifies projectile-like spectator, participant zone, and target-like spectator. In the 200 MeV/nucleon calculations and all calculations in the previous sections Vlasov propagation is nonrelativistic but collisions are treated relativistically (Appendix B of Ref. [19]). Experimental data for ^{124}Sn on ^{119}Sn at 600 MeV/nucleon are available [2]. For 600 MeV/nucleon beam energy, relativistic

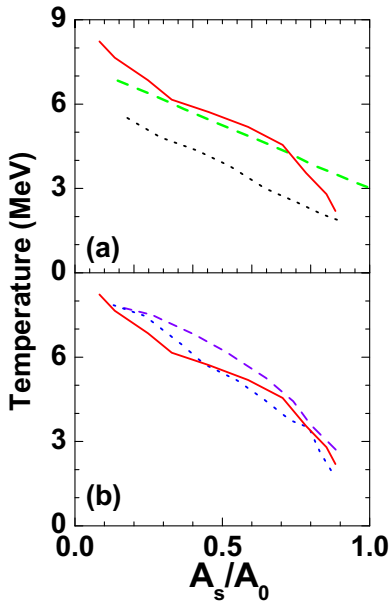

FIG. 7. (Color online) (a) Temperature profile for ^{124}Sn+^{119}Sn reaction at 600 MeV/nucleon obtained from BUU model calculation (red [gray] solid line) compared with that calculated from general formula [Eq. (1)] (green [gray] dashed line) and geometrical model (black dotted line). (b) Temperature profile obtained from BUU calculation for ^{58}Ni+^{181}Ta reaction at 140 MeV/nucleon (violet [gray] dashed line), ^{124}Sn+^{119}Sn reaction at 600 MeV/nucleon (red [gray] solid line) and at 200 MeV/nucleon (blue [gray] dotted line).

kinematics is used for propagation of test particles. This means the following. In the rest frame of each nucleus the Fermi momenta of test particles are calculated in the standard fashion except that once they are generated we treat them like relativistic momenta. Relativistic kinetic energy per nucleon in the rest frame of the nucleus, on the average, becomes only slightly different from the nonrelativistic value (about 0.3 MeV per nucleon). As before, we work in the rest frame of the projectile and the transformation of momenta of test particles of the target to the projectile frame is relativistic. In between collisions, the test particles move with $\dot{\vec{r}} = (\vec{p}c/e_{\rm rel})c$ instead of $\vec{p}/m$. Similarly the change of momentum in test particles induced by the mean field is considered to be the change in relativistic momentum. However, these changes made little difference since in the projectile frame the PLF test particles move slowly.

The 600 MeV/nucleon results are shown in the upper panel of Fig. 7. We show BUU results and compare them with the general formula of Eq. (1). Also plotted are geometric model results. As expected, the geometric model temperatures are lower than those obtained from BUU. In the lower panel of Fig. 7 we plot temperature profiles obtained from BUU calculations for ^{58}NI+^{181}Ta at 140 MeV/nucleon and for ^{124}Sn+^{119}Sn at 200 MeV/nucleon and at 600 MeV/nucleon. Experiments for ^{58}Ni+^{181}Ta at 140 MeV/nucleon were done at Michigan State University.

We return to the discussion of neglecting the pion channel in ^{124}Sn on ^{119}Sn collision at 600 MeV/nucleon. In the early applications of BUU, the pion channel was included by adding the reaction $n + n = \Delta + n$ and the reaction $\Delta + n = n + n$. Number of pions was taken to be the number of Δ's when collisions were over.

We did calculation with this model for a range of impact parameters 2 to 10 fm. For brevity we quote number for $b = 6$ fm. The total number of n_Δ's is not negligible; we estimate this to be about 5 in each event. This number is the sum of n_Δ's in the participant region and n_Δ's in the spectator regions. However, n_Δ in the PLF region is small about 0.1. If we assume that pion emerging from the decay of Δ's in the participant region stays in the participant region and those decaying from Δ's in the PLF stay in the PLF this would mean we get one pion in the PLF in one out of ten events.

Another model would be that when two nucleons collide, occasionally they produce a pion with a given rapidity. Pions with rapidities close to that of the PLF then thermalize in the PLF. The effect on the temperature on the PLF in this model would be very hard to compute. A similar model has been employed to calculate hypernucleus production where a Λ particle is produced in the participant but with a rapidity close to that of the PLF. However, in all the applications we know of, the PLF is assigned an estimated temperature and the modification of temperature due to Λ absorption is not considered [28,29].

V. DISCUSSION

It is quite gratifying that detailed BUU calculations bear out the two striking features of temperature profile in the PLF. These are the following: (a) temperatures are of the order of 6 MeV and (b) there is a very definitive dependence on the intensive quantity A_s/A_0, with temperature falling as this increases.

For large ion collisions the PLF slows down slightly in the laboratory frame (i.e., in the projectile frame it acquires a net small negative velocity). The PLF is excited. Comparison with the geometric model seems to confirm that a large part of the excitation energy owes its origin to nuclear structure effects. The size of the PLF is also larger than what it would be if the PLF were in the ground state. Although the shape was not analyzed, in general, the low-density tail spreads out longer than in nuclei in their ground state.

There are other published works which are related to the physics problem we have investigated here. The closest in spirit and approach is that of Barz *et al.* [30]. The observables which originate from the PLF are often calculated using the SMM model. The starting point of an SMM calculation is the energy E, A_s of the system, which will break up into composites. In SMM these initial conditions are not calculated but chosen so that they fit many experimental data. The BUU calculations in Ref. [30] are done to see if these conditions can be reached for a given impact parameter at a particular time. The example considered was Au on Cu. Our objective here is different. For any pair of heavy ions, we do BUU calculations for many impact parameters b. From BUU calculations at a given b clear indications of participants, target-like spectator, and PLF emerge. The PLF has a mass A_s and an energy E from which we obtain from this BUU calculation. We deduce a temperature using the model described in Ref. [11].

which produces the average energy E. The connection with experiment is through the single empirical formula, Eq. (1). This formula was obtained empirically from data of Sn on Sn at 600 MeV/nucleon but gave good fits to many experimental data for other ion pairs at different energies. There seems to be some advantage to taking a constant temperature for a given b. Constant E for a given b does not seem to work very well [30]. Constant T implies a distribution in E and this appears to work well. There are presumably some differences in the BUU calculations in the earlier pioneering work [30] and here: in choice of inputs for two-body collisions, the mean field, and techniques for Vlasov propagation.

Lastly we make a connection between this work and an earlier work where a fuller description of heavy-ion collision was proposed [31]. In that model there are fast particles simulated by intranuclear model and then pre-equilibrium particle emission (exciton model), leaving a thermalized residual nucleus which undergoes multifragmentation. The BUU simulation is an average description of the reaction in real time. We are only interested in the PLF and it turns out that at the end of 200 fm/c (for Sn on Sn) or 50 fm/c (for Ni on Be), a chump of matter appears which clearly looks like a PLF. In the box where the calculations are done there are many other particles outside the configuration space of the PLF. These will fall under the categories of participants, target spectators (see Sec. III), or in different terminology fast particles, pre-equilibrium particles, etc. There is some ambiguity in our calculation about pre-equilibrium emission. The center of the PLF is quite well located. The choice of the radius is not precisely deducible from the simulation. This has a bearing on the number of pre-equilibrium particles. We estimate that the uncertainty in excitation energy of the PLF is about 1 MeV/nucleon, which may go down if the simulation is carried for a longer period of time.

ACKNOWLEDGMENT

Part of this work was performed at the Variable Energy Cyclotron Centre in Kolkata. S. Das Gupta thanks Dr. D. Srivastava and Dr. A. Chaudhuri for hospitality during a visit at Variable Energy Cyclotron Centre. S. Mallik acknowledges hospitality at McGill for a four-month stay. This work was supported in part by the Natural Science and Engineering Council of Canada.

[1] J. P. Bondorf, A. S. Botvina, A. S. Iljinov, I. N. Mishustin, and K. Sneppen, Phys. Rep. **257**, 133 (1995).
[2] R. Ogul *et al.*, Phys. Rev. C **83**, 024608 (2011).
[3] A. S. Botvina *et al.*, Nucl. Phys. A **584**, 737 (1995).
[4] D. Lacroix, A. Van Lauwe, and D. Durand, Phys. Rev. C **69**, 054604 (2004).
[5] M. Mocko, M. B. Tsang, D. Lacroix, A. Ono, P. Danielewicz, W. G. Lynch, and R. J. Charity, Phys. Rev. C **78**, 024612 (2008).
[6] A. Ono and H. Horiuchi, Prog. Part. Nucl. Phys. **53**, 501 (2004).
[7] J.-J. Gaimard and K.-H. Schmidt, Nucl. Phys. A **531**, 709 (1991).
[8] T. Brohm and K.-H. Schmidt, Nucl. Phys. A **569**, 821 (1994).
[9] K. Summerer and B. Blank, Phys. Rev. C **61**, 034607 (2000).
[10] S. Mallik, G. Chaudhuri, and S. Das Gupta, Phys. Rev. C **83**, 044612 (2011).
[11] S. Mallik, G. Chaudhuri, and S. Das Gupta, Phys. Rev. C **84**, 054612 (2011).
[12] G. Chaudhuri, S. Mallik, and S. Das Gupta, J. Phys.: Conf. Ser. **420**, 012098 (2013).
[13] J. Pochodzalla *et al.*, Phys. Rev. Lett. **75**, 1040 (1995).
[14] S. Das Gupta, A. Z. Mekjian, and M. B. Tsang, Adv. Nucl. Phys. **26**, 91 (2001).
[15] S. Albergo *et al.*, Nuovo Cimento Ser. A **89**, 1 (1985).
[16] C. B. Das, S. Das Gupta, W. G. Lynch, A. Z. Mekjian, and M. B. Tsang, Phys. Rep. **406**, 1 (2005).
[17] S. Das Gupta, S. Mallik, and G. Chaudhuri, Phys. Lett. B **726**, 427 (2013).
[18] S. J. Lee, H. H. Gan, E. D. Cooper, and S. Das Gupta, Phys. Rev. C **40**, 2585 (1989).
[19] G. F. Bertsch and S. Das Gupta, Phys. Rep. **160**, 4 (1988).
[20] J. Gallego, S. Das Gupta, C. Gale, S. J. Lee, C. Pruneau, and S. Gilbert, Phys. Rev. C **44**, 463 (1991).
[21] R. J. Lenk and V. R. Pandharipande, Phys. Rev. C **39**, 2242 (1989).
[22] S. E. Koonin *et al.*, Phys. Rev. C **15**, 1359 (1977).
[23] W. H. Press *et al.*, in *Numerical Recipes* (Cambridge University Press, Cambridge, UK, 1986), pp. 615–667.
[24] R. S. Varga, *Matrix Iterative Analysis* (Springer, Berlin, 2000).
[25] H. Feldmeier and P. Danielewicz, MSUCL-833 (1992).
[26] W. D. Myers, Nucl. Phys. A **296**, 177 (1978).
[27] G. Cecil, S. Das Gupta, and W. D. Myers, Phys. Rev. C **22**, 2018 (1980).
[28] V. Topor Pop and S. Das Gupta, Phys. Rev. C **81**, 054911 (2010).
[29] A. S. Botvina and J. Pochodzalla, Phys. Rev. C **76**, 024909 (2007).
[30] H. W. Barz *et al.*, Nucl. Phys. A **561**, 466 (1993).
[31] A. S. Botvina and I. N. Mishustin, Phys. Lett. B **294**, 23 (1992).